Journal of Engineering Physics and Thermophysics, Vol. 82, No. 5, 2009

PHYSICAL MODEL OF ENERGY ACTIVATION OF ANODE MICROARC OXIDATION

N. M. Chigrinova,[a] A. A. Kuleshov,[b] and V. V. Nelaev[c]

UDC 691.9.048.4

A physical-mathematical model of energy intensification of the microplasma-spark treatment of a material in a liquid by passing ultrasonic waves through it is proposed. The conditions of ultrasound action and its parameters as well as the characteristics of the liquid medium carrying an electric pulse were determined for optimization of the cavitation and energy action on the modification and hardening of "venting" materials in the process of their anode microarc oxidation. An analysis of the results of simulation of the physical effects arising in the process of anode microarc oxidation of materials under the indicated conditions has shown that this process can be controlled for the purpose of obtaining definite-thickness and quality coatings by searching for an external ultrasound action with a certain amplitude and frequency and an electrolyte possessing special characteristics determined by its density, viscosity, and the presence of particles with a definite degree of dispersion.

Keywords: *microarc oxidation, modification process, coatings, energy intensification, ultrasound action, simulation of physical effects, physical-mathematical model, cavitation bubbles, Rayleigh–Plesset equation, amplitude, frequency, electrolyte characteristics.*

Introduction. A new promising direction of increasing the service life and quality of products without marked increase in their prime cost is the surface hardening and modification of materials from which they are made with the use of microplasma-arc methods, one of which is anode microarc oxidation (AMAO). This technology makes it possible to obtain various high-adhesion coatings on the surfaces of different-size and application products made from "venting" materials.

Formulation of the Problem. The aim of the present work is to investigate the problems on intensification of energy and mass transfer in the process of anode microarc oxidation of materials, minimization of the energy expended for this process, and optimization of the parameters of the process for the purpose of obtaining of composite coatings with uniformly distributed stresses and a regular structure.

Since the formation of coatings by microplasma-arc methods (one of which is the AMAO method) based on the synergetics laws is determined by many factors and an efficient methodology for control of the dynamics of this process and the quality of the coatings obtained is absent, there is a need for development of theoretical representations on the effects arising in the substrate–material–coating system under different internal and external actions for determining measures on intensification of the energy and mass transfer in this system in the process of its anode microarc oxidation and optimization of the parameters of the process for minimization of the energy expended for it and obtaining composite coatings with uniformly distributed stresses and a regular structure.

We present a physical model defining the kinetics of energy and mass transfer in the process of anode microarc oxidation of materials conducted with intensification of the formation of coatings by different methods providing a change in the state and composition of an electrolyte [1, 2]:

a) chemical intensification realized with the use of special ingredients, introduced into a standard electrolyte, that are capable of increasing the rate of the chemical reactions between the oxidized metal and the electrolyte-electrolysis products, decreasing the viscosity of the electrolyte, and be the seeds of new oxidation phases;

[a]Institute of Welding and Protective Coatings, State Scientific Institution "Institute of Powder Metallurgy," National Academy of Sciences of Belarus, 12 B Platonov Str., Minsk 220005, Belarus; [b]Belarusian State University, 4 Nezavisimost' Ave., Minsk, 220030; [c]Belarusian State University of Information and Radio Engineering, 6 P. Brovka Str., Minsk, 220013, Belarus. Translated from Inzhenerno-Fizicheskii Zhurnal, Vol. 82, No. 5, pp. 1004–1013, September–October, 2009. Original article submitted February 2, 2009; revision submitted April 4, 2009.

 1062-0125/09/8205-1014©2009 Springer Science+Business Media, Inc.

b) electric intensification realized by introduction of charged dispersed particles into an electrolyte for activation and structurization of it;

c) mechanical intensification changing the state of an electrolyte by external ultrasound action.

Model Used. *Cavitation as a mechanisms of intensification of the AMAO process under an external ultrasound action.* The ultrasound intensification of the AMAO process for the purpose of increasing the rate of formation and growth of oxide coatings is based on the cavitation effects arising in a liquid in which ultrasonic vibrations of definite intensity are excited.

Cavitation (from the Latin "kavitas"–cavity) represents the formation of gas, vapor, or vapor-gas bubbles in a liquid, which is favorable to the propagation of ultrasonic vibrations in the liquid and a high-energy release. Cavitation bubbles appear in the regions of the liquid where the pressure is lower than the critical one P_{cr} (in a real liquid, P_{cr} is approximately equal to the pressure of the saturated vapor of this liquid at a given temperature). Acoustic cavitation arises in a liquid subjected to a sound or ultrasound action of frequency from 20 kHz to 10 MHz, which takes place in the case of mechanical intensification of anode microarc oxidation. An ultrasonic wave passing through an electrolyte gives rise to pulsations in it: an expansion (a negative pressure) and a compression (positive pressure). If the intensity (amplitude) of the sound field is fairly high, the ultrasound can cause the formation, growth, and rapid compression of saturated-vapor bubbles. The collapse of a compressed bubble leads to a local powerful release of heat energy, a sharp increase in the pressure, and intensification of the high-energy chemical processes. These processes indicate that ultrasound intensification of the AMAO process can be used for increasing the rate of formation and growth of oxide coatings. Therefore, we developed a model for optimization of the regimes of ultrasound action on the dynamics of anode microarc oxidation and, consequently, on all interaction processes occurring in an activated electrolyte.

The principles of the cavitation mechanisms were theoretically investigated and the possibilities of use of cavitation in technological processes were considered in [3–5]. Acoustic oxidation, unlike hydrodynamic oxidation, arises in an electrolyte when ultrasonic waves with a high amplitude exceeding any threshold value pass through it. Cavitation bubbles are formed during the half-period of the rarefaction on the so-called cavitation seeds, which serve as gas inclusions most often; these inclusions are contained in the liquid and on the vibrating surface of an acoustic radiator or on the impurities introduced specially into the liquid in the case of both chemical and electric intensification of the AMAO process. Cavitation bubbles collapse during the half-period of the compression and, in doing so, give rise to short-duration (10^{-6} sec) pulses of pressure of up to 10^8 Pa and higher.

The sound field causing cavitation in an electrolyte is spatially inhomogeneous, especially in the case of introduction of additional chemical and other ingredients into the electrolyte. Because of this, along with pulsations, a bubble executes a translatory motion in the liquid. The direction of motion of a bubble in a standing ultrasonic wave is determined by the ratio between its initial and finite radii and the natural-vibration frequency that is equal to the ultrasonic-wave frequency [6]. In the case where the bubble radius is smaller than the resonance one ($R < R_{res}$), bubbles pulsate in phase with the pressure oscillations and migrate in the direction to the pressure antinode, and, at $R > R_{res}$, bubbles move to the pressure nodes. The rate of translatory motion of the bubbles found in the ultrasound field with an acoustic pressure P_a also depends on the properties of the liquid — the kinematic-viscosity coefficient and the surface tension. The translatory motion of bubbles is the reason for their coagulating growth. The appearance of cavitation and the degree of its development are characterized quantitatively by the so-called cavitation number

$$C = (p_{stat} - p_s)/A \, .$$

Cavitation differs from ordinary boiling in that, when the velocity of the liquid flow relative to the body increases, the pressure of the flow decreases to the pressure of the saturated vapor. In this case, the liquid comes to a boil and cavitation vapor-gas bubbles of microscopic sizes are formed. These bubbles enter the increased-pressure region formed, e.g., as a result of the electric intensification of the electrolyte by additional introduction of charged polyradicals into it [7]. These polyradicals playing the role of additional minicathodes give rise to the secondary electric field and serve to increase its pressure near the oxidized metal. As a result, the bubbles collapse (are condensed) with the formation of cumulative jets converging to points. At individual points in these numerous local regions, the cumulative effects cause a point increase in the pressure to tens of thousands of atmospheres and in the temperature

to tens of thousands. Moreover, the sudden disappearance of cavitation bubbles leads to the formation of hydraulic shocks and, as a consequence, of ultrasonic compression and expansion waves in the liquid. If a shock wave comes up against an obstacle, it breaks down its surface. This effect makes for obtaining of a high-density coating because the upper growing layers of the film subjected to such destruction have a porous and inhomogeneous structure. The energy of the collapsed bubbles is expended not only for the formation of shock waves, but also for the local heating of the gas contained in the compressed cavitation pockets and the formation of free radicals intensifying the chemical reactions and increasing the rate of growth of oxide layers.

The combined action of the cumulative jets, the hydrodynamic shocks, and the ultrasound field provides sterilization of the liquid being treated and emulsification of the products that are usually immiscible in continuously changing complex systems like an electrolyte. In this case, the chemical reactions are intensified, the solid particles dispergate to the micron level in the solution and can become new centers of formation of bubbles, and the product subjected to anode microarc oxidation homogenizes with the formation of a high-quality coating on it.

Energy realized as a result of the collapse of a cavitation bubble. The energy released in the process of collapse of cavitation bubbles under an external ultrasound action is limited. The release of this energy in the form of light was discussed in detail from the sonoluminescence standpoint in [8–10]. It was concluded based on the experimental and theoretical investigations that the energy released as a result of the collapse of a cavitation bubble depends first of all on the ratio R_{max}/R_0 [11, 12]. The size of the germ is determined by the concentration of the gas inclusions in the liquid and the sizes of the dissolved solid particles that also serve as centers of formation of cavitation bubbles. In the AMAO process, such centers can be charged polyradicals, providing electric intensification of the anode microarc oxidation, and finely dispersed chemical ingredients, causing chemical intensification of this process. The R_{max}/R_0 value is determined by the external dynamic parameters (in particular by the ultrasound amplitude and frequency) and the intrinsic physical properties of the liquid (its density, viscosity, surface tension, and the velocity of sound in it).

The potential energy U released as a result of the collapse of a bubble of radius R_{max} can be written with a high degree of approximation in the form

$$U = P_c\left(\frac{4}{3}\pi R_{max}^3\right). \tag{1}$$

This energy is distributed between the atoms and molecules of the gas in the bubble and is released as a result of its collapse. On the assumption that the gas in the bubble of radius R_0 is under ordinary equilibrium conditions, the number of atoms or molecules in this bubble can be estimated at N_0. It is apparent that N_0 is proportional to the volume of the bubble $V = \frac{3}{4}\pi R_0^3$. It follows herefrom that the energy density, i.e., the energy per molecule or atom, is determined by the simple expression

$$E_d = U/N_0 = 0.025\ (P_c/P_0)\ (R_{max}/R_0)^3\ . \tag{2}$$

For the polytropic process in which the pressure and volume of ideal gas are related as pV^k = const, the expression for E_d can be written in the form

$$E_d = 0.025\left(\frac{R_{max}^3}{R_0^3}\right)\left[\frac{1}{1 + k\left(\frac{P_c}{P_0}\right)\left(\frac{R_{max}^3}{R_0^3}\right)}\right]. \tag{3}$$

If the pressure P_c at the instant a bubble collapses is equal to the pressure of the surrounding liquid P_0, $E_d = 0.025\ (R_{max}/R_0)^3$ and the density of the energy released in the process of collapse of the bubble under an external ultrasound action will be only a function of the ratio R_{max}/R_0. For example, in the case where the expansion coeffi-

cient of a bubble is equal to 10, which is typical for the one-bubble collapse, the energy density is equal to 25 eV per atom or molecule. The larger the radius of the collapsed bubble, the higher the energy released in the process of its collapse.

In [11], the temperature T_g and pressure P_g inside a collapsing bubble of radius $R(t)$ was estimated based on the solution of the Rayleigh–Plesset equation for a pulsating bubble and the adiabatic equation of state for the gas inside a uniformly compressed bubble at a pressure P_g and a temperature T_g:

$$T_g(R) = \frac{T_0 R_0^{3(\gamma-1)}}{(R^3 - a^3)^{\gamma-1}}, \quad P_g(R) = \frac{P_0 R_0^{3\gamma}}{(R^3 - a^3)^{\gamma}}. \tag{4}$$

For a slowly pulsating bubble, $T_g \approx T_0$. Theoretical estimations have shown that the temperature inside such a bubble can reach 10^8 K.

Models of dynamics of cavitation bubbles under external ultrasound action. The majority of works devoted to the dynamics of development of cavitation bubbles are based on the solution of the classical Rayleigh–Plesset equation representing a form of the moment-conservation equation. It describes the behavior of an isolated spherical bubble of homogeneous composition in an infinite liquid medium in the absence of heat-and-mass-transfer effects. At a later time, different modifications of the initial model were developed for the purpose of removal of the indicated restrictions. First and foremost, this concerns the estimation of the thermodynamic and transport effects [11]. In [12–14] where models of "clouds" (clusters) of bubbles were considered, it has been shown that the energy released by clusters of oscillating bubbles is concentrated at their centers. This phenomenon was considered in the model accounting for the additional effect arising due to the reaction of radicals [9, 15]. The influence of the environment on the dynamics of cavitation bubbles is taken into account in the models described in [16]. A comparative analysis of the experimental results and theoretical data obtained with the use of different models was performed in [11].

The Rayleigh–Plesset equation (more precisely its Noltingk–Neppiras–Poritsky modification) is especially nonlinear. In actual fact it is an example of description of a chaotic dynamic system [17, 18]. An analysis of the nonlinear dynamics of a bubble in an acoustic field consisting of high-power harmonic and noise components has shown that the influence of the stochastic component is significant in the region where the dynamic states of the bubble are bistable. Its behavior in this region is characterized by the substantial increase in the duration of the transient processes and the essentially non-Gaussian distribution of the fluctuations near the stable trajectories.

The characteristic form of the Rayleigh–Plesset equation is as follows:

$$\frac{p_s(T_\infty) - p_\infty(t)}{\rho_{liq}} + \frac{p_{g0}}{\rho_{liq}}\left(\frac{R_0}{R}\right)^{3k} = R\ddot{R} + \frac{3}{2}(\dot{R})^2 + \frac{4\mu_{liq}\dot{R}}{R} + \frac{2S}{\rho_{liq}R}, \quad p_\infty(t) = p_{stat} + A\sin(2\pi ft). \tag{5}$$

An external ultrasound action is defined by the term $p_\infty(t) = p_{stat} + A\sin(2\pi ft)$. It is apparent that Eq. (5) is nonlinear and has no analytical solution. Substitution of the variables (e.g., as in [19])

$$\dot{R} = u, \quad \dot{\Theta} = f \tag{6}$$

gives the expression

$$\dot{u} = \frac{p_s(T_\infty) - p_{stat} - A\sin(2\pi\Theta)}{\rho_{liq}R} + \left(\frac{p_{g0}}{\rho_{liq}R}\right)\left(\frac{R_0}{R}\right)^{3k} - \frac{3}{2}\frac{u^2}{R} - 4\mu_{liq}\frac{u}{R^2} - \frac{2S}{\rho_{liq}R^2}. \tag{7}$$

However, Eq. (5) in the Rayleigh–Plesset model takes no account of the compressibility of the liquid — the effect that should appear in the case of collapse of cavitation bubbles at a high pressure. This drawback is absent in the Keller–Miksis model [20] and in its modification made by Parlitz and his co-authors [17, 21] that is defined by the equation

$$\left(1 - \frac{\dot{R}}{c}\right)R\dot{R} + \frac{3}{2}\dot{R}^2\left(1 - \frac{\dot{R}}{3c}\right) = \left(1 - \frac{\dot{R}}{c}\right)\frac{P}{\rho_{liq}} + \frac{R}{\rho_{liq}c}\dot{P}, \tag{8}$$

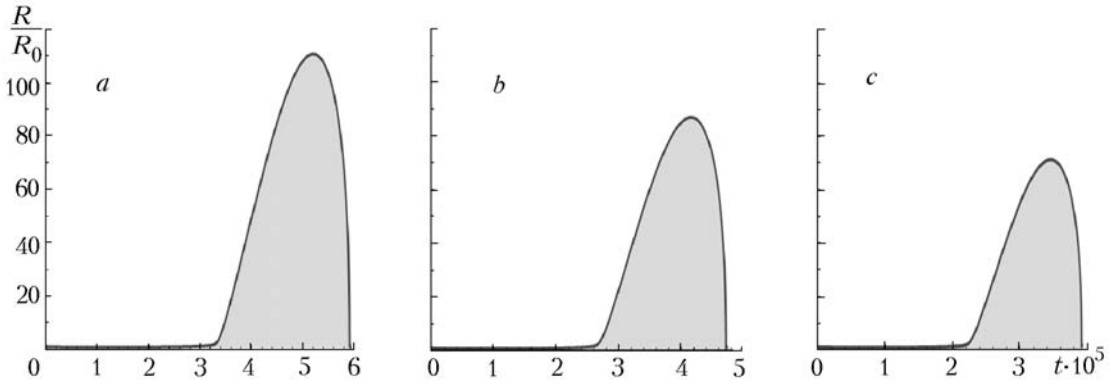

Fig. 1. Change in R/R_0 with time under the action of an ultrasonic wave with an amplitude A = 2 bar and a varying frequency f at R_0 = 1 μm: a) f = 20 kHz, R_{max}/R_0 = 110.7; b) 25 and 86.9; c) 30 and 71.2. t, min.

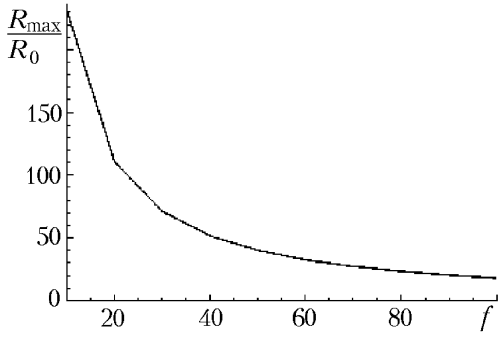

Fig. 2. Dependence of R_{max}/R_0 on the frequency f of the external ultrasound action at R_0 = 1 μm and A = 2 bar. f, kHz.

where

$$P = \left[p_{stat} - p_s(T_\infty) + \frac{2S}{R_0}\right]\left(\frac{R_0}{R}\right)^{3k} - \frac{2S}{R} - \frac{4\mu_{liq}\dot{R}}{R} - p_{stat} + p_s(T_\infty) - A\sin(2\pi ft). \quad (9)$$

Substitution of variables (6), by analogy with (5), reduces (8) to the equation

$$\dot{u} = \left[\left(1 - \frac{u}{c}\right)R + \frac{4\mu_{liq}}{\rho_{liq}c}\right]^{-1}\left[-\frac{u^2}{2}\left(3 - \frac{u}{c}\right) + \left(1 + (1-3k)\frac{u}{c}\right)\left(\frac{p_{stat} - p_s(T_\infty)}{\rho_{liq}} + \frac{2S}{\rho_{liq}R_0}\right)\left(\frac{R_0}{R}\right)^{3k}\right.$$
$$\left. - \frac{2S}{\rho_{liq}R_0} - \frac{4\mu_{liq}u}{\rho_{liq}R} - \left(1 + \frac{u}{c}\right)\frac{p_{stat} - p_s(T_\infty) + A\sin(2\pi\Theta)}{\rho_{liq}} - R\frac{2\pi f}{\rho_{liq}c}A\cos(2\pi\Theta)\right]. \quad (10)$$

Thus, the above theoretical representations of the factors influencing the cavitation processes arising in an electrolyte under the action of ultrasound create prerequisites for performance of computational optimizational investigations for the purpose of working-out of recommendations on the intensification of the energy and mass transfer in the process of microarc oxidation of materials.

Results of Simulation of the Growth and Collapse of Cavitation Bubbles in an Electrolyte through Which Ultrasonic Waves Propagate. The main challenge of computational optimizational investigations is to determine the parameters of an external ultrasound action (its frequency and amplitude) providing a necessary energy release in the process of collapse of cavitation bubbles. This will allow one to select the conditions necessary for control over the intensification of the anode microarc oxidation of materials.

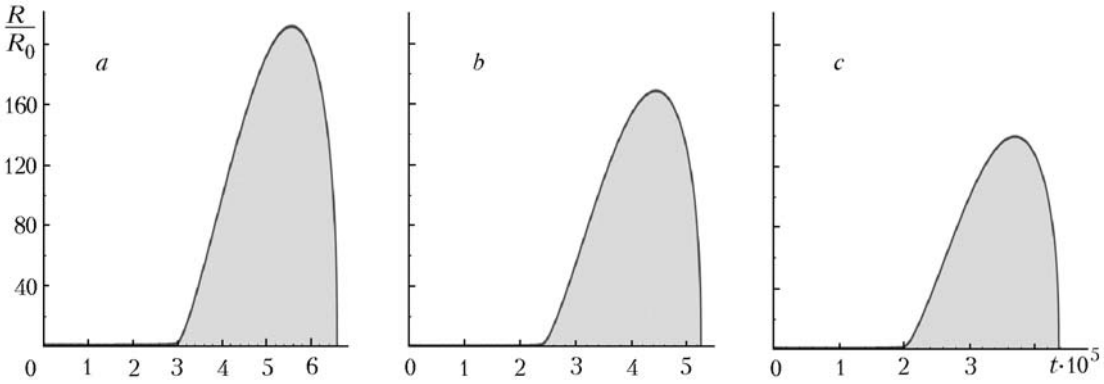

Fig. 3. Change in R/R_0 with time under the action of an ultrasonic wave with an amplitude A = 3 bar and a varying frequency f at R_0 = 1 μm: a) f = 20 kHz, R_{max}/R_0 = 212.1; b) 25 and 168.6; c) 30 and 139.8. t, min.

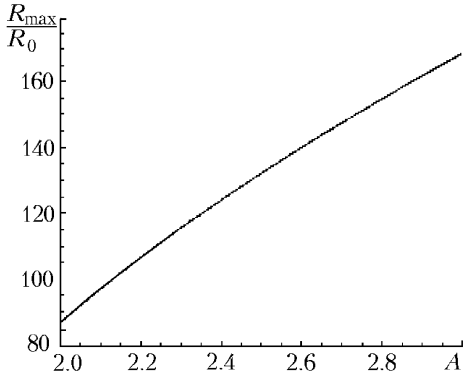

Fig. 4. Dependence of R_{max}/R_0 on the amplitude A at f = 25 kHz and R_0 = 1 μm. A, bar.

Below are results of investigation of the dependence of the ratio R_{max}/R_0 on the parameters of an external ultrasound action A and f, the initial radius of a cavitation bubble (determined by the type and size of the germs), and the physical properties of the electrolyte (its density ρ and viscosity μ and the external pressure p_{stat}) — the parameters with which one can control the intensity of the microarc oxidation of a material.

The numerical calculations were carried out with the use of the Rayleigh–Plesset model, its Keller–Miksis–Parlitz modification (Eqs. (8) and (10)), and *Mathematica* software.

In the calculations we used standard physical parameters and constants concerning the effects arising in an electrolyte: S = 0.073 J/m^2; μ = 0.9 P, ρ = 0.998 g/cm^3, c = 1500 m·sec^{-1}, $p_s = 2.34 \cdot 10^3$ bar, p_{stat} = 1.01325 bar.

The density of the energy released is proportional to $(R_{max}/R_0)^3$; however, this ratio depends on the physical properties of the solution and the initial radius of a bubble R_0. The value of R_0 is determined by the conditions of formation of bubbles, i.e., the nature and size of the centers of their nucleation (in particular by the size of the polyradicals introduced into the electrolyte in the process of its electric intensification) and the statistical size distribution of bubbles. The results of variational calculations of the time dependence of R/R_0 at constant values of R_0 and the amplitude A are presented in Fig. 1. From the graphs presented, it is clearly seen that R_{max}/R_0 is related to f in the range of its change being investigated: the value of R_{max}/R_0 decreases by almost 1.5 times (from 110.7 to 71.2) when the frequency increases from 20 to 30 kHz. This conclusion is supported by the data presented in Fig. 2 where the dependence of R_{max}/R_0 on the frequency f at R_0 = 1 μm and A = 2 bar is shown.

Figure 3 illustrates the time dependence of R/R_0 at different values of f, a constant value of R_0, and a larger value of A = 3 bar. Comparison of Figs. 1 and 3 shows that an increase in the amplitude A of an ultrasound action by 1.5 times (from 2 to 3 bar) in the case where its frequency remains unchanged leads to an increase in the ratio R_{max}/R_0 by almost two times, which is supported by the results presented in Fig. 4.

TABLE 1. Dependence of R_{max}/R_0 on the Amplitude A and Frequency f of the Ultrasound Action at a Fixed Initial Radius of a Bubble R_0 = 1 μm

A, bar	f, kHz		
	20	25	30
2	110.7	86.9	71.2
3	212.1	168.6	139.8

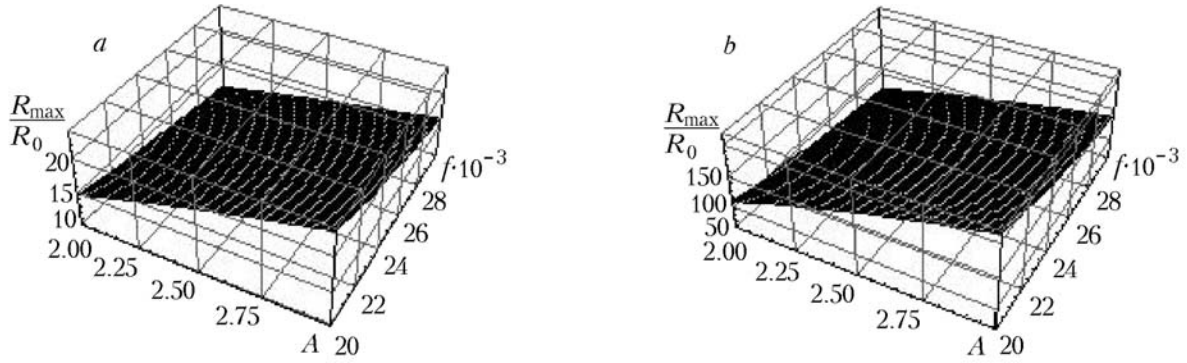

Fig. 5. Dependence of R_{max}/R_0 on the frequency f and amplitude A at R_0 = 10 (a) and 1 μm (b). A, bar; f, Hz.

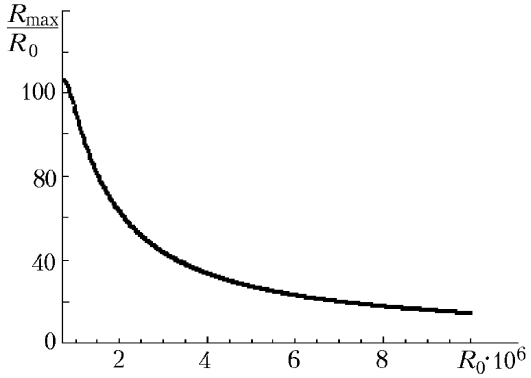

Fig. 6. Dependence of R_{max}/R_0 on the initial radius of a cavitation buble R_0 at constant values of the amplitude A = 2 bar and the frequency f = 20 Hz. R_0, μm.

Table 1 presents summary data obtained from the analysis of Figs. 1 and 3. It is seen that throughout the above-indicated range of frequencies the dependence of R_{max}/R_0 on the amplitude and frequency of an ultrasound action leads to an almost 2-fold increase in R_{max}/R_0 and a 8-fold increase (see Eqs. (3) and (4)) in the energy released as a result of the collapse of cavitation bubbles.

As is seen from Fig. 2, the strong dependence of R_{max}/R_0 on f takes place only at the beginning of the ultrasonic-frequency range — at frequencies lower than 40 kHz, and then it decreases monotonically and smoothly with increase in f. The reverse dependence of R_{max}/R_0 on the amplitude A (R_{max}/R_0 increases with increase in A (Fig. 4)) allows one to solve the problem on determination of the optimum ranges of change in A and f of an ultrasound action within the limits of which the ratio R_{max}/R_0 necessary for control of the AMAO intensity is provided.

One further "degree of freedom" for control of the AMAO process is the initial radius of a bubble R_0 determined by the conditions of germ formation, in particular by the sizes of charged particles having different degrees of dispersion introduced into the electrolyte. Figure 5 shows the dependence of R_{max}/R_0 on the frequency f and the amplitude A of an ultrasound action at different values of R_0, and, in Fig. 6, the dependence of R_{max}/R_0 on R_0 at constant values of A and f is presented.

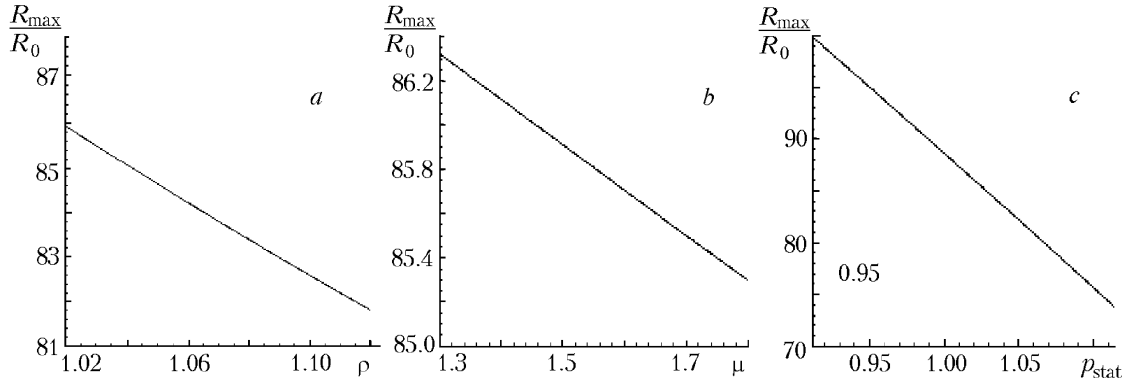

Fig. 7. Dependence of R_{max}/R_0 on the state of the electrolyte at A = 2 bar, f = 20 Hz, and R_0 = 1 μm: a) on the density ρ at μ = 0.9 P and p_{stat} = 1 bar; b) on the viscosity μ at ρ = 0.998 g/cm^3 and p_{stat} = 1 bar; c) on the external pressure p_{stat} at ρ = 0.998 g/cm^3 and μ = 0.9 P. ρ, g/cm^3; μ, P; p_{stat}, bar.

TABLE 2. Density and Viscosity of the Electrolyte Versus Its Actual Acidity

Parameter	Medium		
	normal	acidic (20% H_2SO_4)	alkali (10% NaOH)
ρ, g/cm^3	0.998	1.15	1.25
μ, P	0.9	1.38	1.86

TABLE 3. Results of Solution of the Optimization Problem on Determination of the Admissible Spread in the Input Parameters ρ, μ, and p_{stat} Providing a Definite Range of Change in the Output Parameters R_{max}/R_0

R_{max}/R_0	ρ, g/cm^3	μ, P	p_{stat}, bar
100 ± 10%	{0.699 – 1.297}	{0.71 – 1.32}	{0.80 – 1.32}
300 ± 15%	{0.634 – 1.567}	{0.53 – 1.05}	{0.50 – 1.90}

The curve in Fig. 6 shows that the ratio R_{max}/R_0 has a maximum value in a fairly narrow, even if real from the practical realization standpoint, range of change in $R_0 \sim$ 1–3 μm; this value is of the same order of magnitude as the size of the introduced polyradical particles that are most probable centers of nucleation of cavitation bubbles.

It should be noted that R_0 can influence differently the energy released as a result of the collapse of bubbles. On the one hand, the smaller the initial radius of a particle, the larger the ratio between its final and initial radii, i.e., the higher the energy released. On the other hand, the density of the energy released in smaller bubbles is smaller because the number of particles in the vapor phase of a collapsing bubble, responsible for the high-power energy release, is smaller. This is explained by the dependence relating the density N_0 of these particles to the radius of the bubble: $N_0 \sim (R_0)^{1/3}$.

As is seen from the initial Rayleigh–Plesset equation, the level of the energy release depends not only on the parameters of the external ultrasound action and the initial size of a cavitation bubble, but also on the properties of the electrolyte (its density ρ and viscosity μ) and the constant external pressure p_{stat}.

Figure 7 presents the dependences of R_{max}/R_0 on ρ, μ, and p_{stat} at A = 2 bar, f = 20 kHz, ρ = 0.998 g/cm^3, μ = 0.9 P, and p_{stat} = 1 bar.

The data presented in Table 2 on the density and viscosity of the electrolyte versus its acidity point to fairly wide ranges of change in ρ (from 0.998 to 1.25 g/cm^3) and μ (from 0.9 to 1.86 P), which allows one to search for an electrolyte of definite composition and type to control the energy release in the process of collapse of bubbles.

Optimization of the parameters of the above-described multifactor problem is associated with determination of the range of change in the input characteristics (the density and viscosity of the electrolyte, the external pressure) at which the output characteristic R_{max}/R_0 will take definite values. The optimization problem was solved in the re-

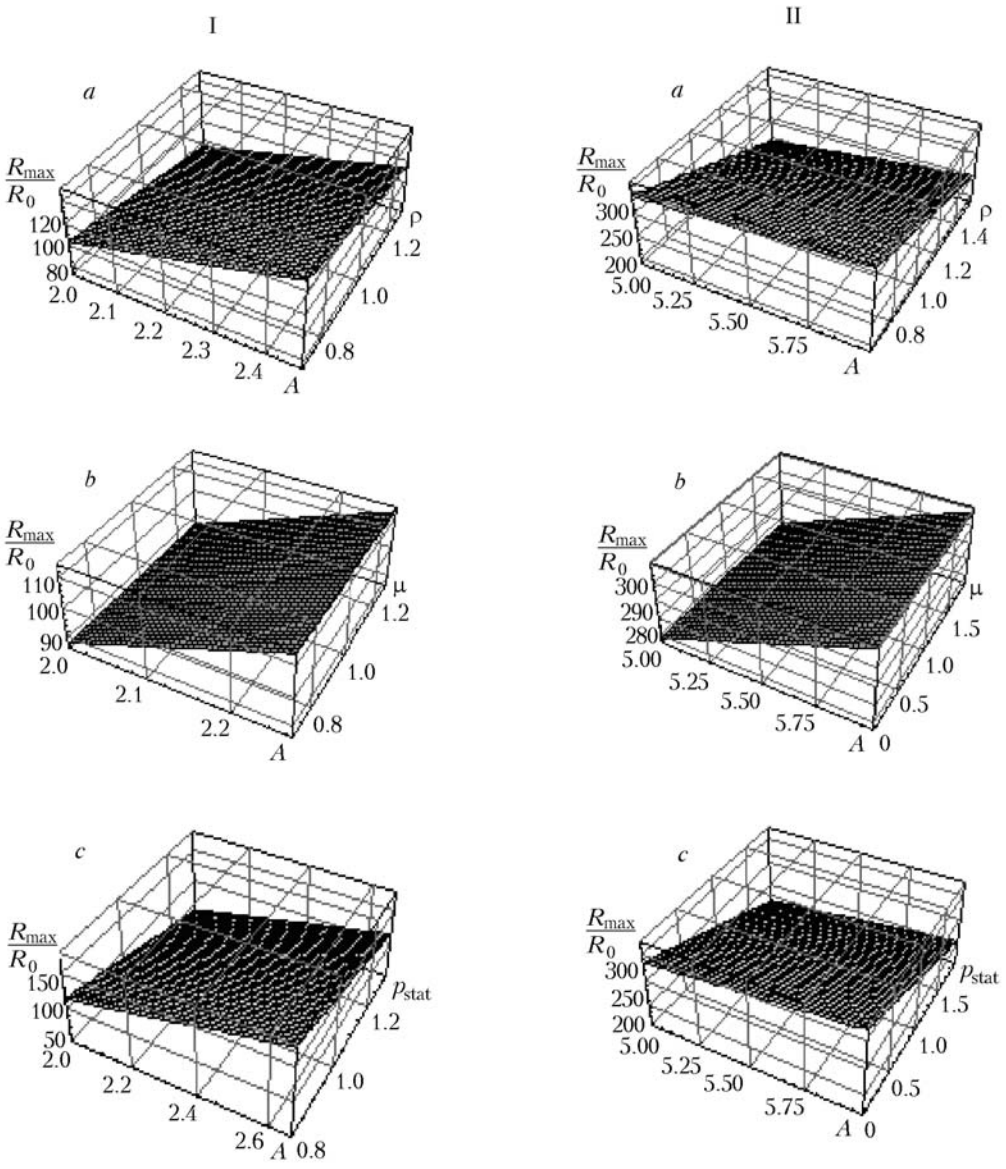

Fig. 8. Dependence of R_{max}/R_0 taking values 100 ± 10% (I) and 300 ± 15% (II) on the amplitude of the ultrasound action A and the state of the electrolyte at f = 25 kHz and R_0 = 1 μm: a) on the density ρ at μ = 0.9 P and p_{stat} = 1 bar; b) on the viscosity μ at ρ = 0.998 g/cm^3 and p_{stat} = 1 bar; c) on the external pressure p_{stat} at ρ = 0.998 g/cm^3 and μ = 0.9 P. A, p_{stat}, bar; μ, P; ρ, g/cm^3.

sponse-surface approximation [22] used mainly for obtaining of a polynomial approximating the dependence of the outer characteristics on the input factors. Figure 8 presents the surfaces of the response R_{max}/R_0 in the region where R_{max}/R_0 = 100 ± 10% and R_{max}/R_0 = 300 ± 15% in the spaces (A, ρ), (A, μ), and (A, p_{stat}) constructed with the use of the polynomial dependence R_{max}/R_0 on ρ, μ, and p_{stat}, calculated by the response-surface methodology. The approximation dependence obtained (the correlation coefficient is equal to 0.99) allowed us to determine the permissible intervals of change in the parameters ρ, μ, and p_{stat}, in which R_{max}/R_0 takes definite values. Table 3 presents results of two optimization calculations differing by the prescribed values (100 and 300) of the ratio R_{max}/R_0 and the ranges of spread in this quantity (±10% and ±15%). It should be noted that R_{max}/R_0 = 300 only in the case of ultrasound action with an amplitude of 5–6 bar (see Fig. 8).

Comparison of the data presented in Tables 2 and 3 allows the conclusion that the permissible-viscosity range 0.634–1.567 P obtained for $R_{max}/R_0 = 300 \pm 15\%$ corresponds to the interval of possible viscosity values 0.9–1.86 P (depending on the acidity of the solution), which cannot be said about the electrolyte density: the corresponding ranges of change in ρ are 0.634–1.567 g/cm^3 and 0.998–1.25 g/cm^3.

Conclusions. A physical model defining the intensification of energy and mass transfer in the process of anode microarc oxidation of a material was proposed. This model explains the intensification of the indicated processes by a high energy released as a result of the collapse of cavitation bubbles formed in the electrolyte under an external ultrasound action. The mathematical description of this phenomenon is based on the modified hydrodynamic Rayleigh–Plesset equation that is numerically realized with the use of *Mathematica* software. The calculation data obtained using the model proposed indicate that the AMAO technology can be controlled for the purpose of formation of definite-thickness and quality coatings by searching for an external ultrasound action with a certain amplitude and frequency, an electrolyte found in a certain state determined by its density, viscosity, and the existence of polyradicals of definite size in it, and an external constant pressure.

NOTATION

A, amplitude of acoustic vibrations; a, radius of a gas bubble compressed to such a degree that the distance between the atoms/molecules in it is equal to the van der Waals radius; C, number of a cavitation; c, velocity of sound in the liquid; E_d, energy per molecule or atom in a cavitation bubble; f, frequency of an ultrasonic wave; k, polytropic constant; N_0, number of atoms or molecules in a cavitation bubble of radius R_0; p, current pressure in a cavitation bubble; P_0, initial pressure prior to the growth of a bubble; P_c, pressure of the surrounding medium at the beginning of collapse of a bubble that can be considered as the collapse pressure; P_{cr}, critical pressure in the liquid determining the lower threshold of formation of cavitation bubbles; P_a, acoustic pressure; P_g, pressure of a uniformly compressed bubble; p_{g0}, partial pressure of the gas in a bubble of radius R_0; p_s, pressure of the saturated vapor; p_∞, pressure in the liquid at a large distance from the bubble; p_{stat}, hydrostatic pressure outside the bubble; R, radius of a cavitation bubble; R_{max}, maximum radius of a bubble attained by it for the half-period of expansion of the liquid under an ultrasound action; R_0, initial radius of a cavitation bubble whose size is determined by the bubble-germ size; R_{res}, resonance radius of a cavitation bubble; S, surface tension coefficient of the liquid; T_0, temperature of the surrounding medium; T_∞, temperature of the liquid at a large distance from the bubble; T_g, temperature of a uniformly compressed bubble; V, volume of a cavitation bubble; t, time; U, potential energy released as a result of the collapse of a bubble; u, ratio of heat capacities C_p/C_v (at a constant pressure and volume); μ, viscosity of the liquid; ρ_{liq}, density of the liquid; Θ, argument introduced as a new variable for solving Eq. (5). Subscripts: a, acoustic; c, collapse; cr, critical; d, density; g, gas; g_0, gas at R_0; liq, liquid; max, maximum; res, resonance; s, saturation; stat, static; points above symbols, derivatives with respect to time.

REFERENCES

1. N. M. Chigrinova, V. E. Chigrinov, and A. V. Drozdov, Optimization of technological methods of microplasma-arc action for development of energy-saving processes of the formation of protective coatings, in: *Welding and Related Technologies*, *Collected papers of Int. Symposium*, Belorusskaya Nauka, Minsk (2008), pp. 48–52.
2. N. M. Chigrinova, A method of intensification of the process of formation of oxide coatings by anode microwave oxidation in weak alkali solutions with minimization of the energy expended, Application No. A20081239 of 30.09.2008.
3. J. Daily and D. Harleman, *Fluid Mechanics* [Russian translation], Énergiya, Moscow (1971).
4. R. Knapp, J. Daily, and F. Hammitt, *Cavitation* [Russian translation], Mir, Moscow (1974).
5. V. V. Rozhdestvenskii, *Cavitation* [in Russian], Énergiya, Moscow (1977).
6. A. D. Al'tshul', *Hydraulics and Aerodynamics* [in Russian], Mir, Moscow (1987).

7. N. M. Chigrinova, Combination of microplasma-arc methods of treatment under the conditions of a regular discharge for formation of oxide-ceramic coatings on objects from "venting" and ferrous metals, in: *Proc. 27th Annual Int. Scientific-Practical Conf. and Blitz-Exhibition "Composite Materials in Industry"* [in Russian], Yalta (2007), pp. 240–243.
8. M. A. Margulis, *Sonochemistry and Cavitation*, Gordon and Breach, London (1995).
9. V. Kamath, A. Prosperetti, and F. Egolfopoulos, A theoretical study of sonoluminescence, *J. Acoust. Soc. Am.*, **94**, No 1, 248–260 (1993).
10. S. Putterman, P. G. Evans, G. Vazquez, and K. Weninger, Cavitation science: Is there a simple theory of sonoluminescence? *Nature*, **409**, 782–783 (2001).
11. C. E. Brennen, *Cavitation and Bubble Dynamics*, Oxford University Press, Inc., Madison Avenue, New York (1995).
12. Y. Matsumoto and S. Yoshizawa, Behaviour of a bubble cluster in an ultrasound field, *Int. J. Numer. Meth. Fluids*, **47**, Nos. 6–7, 591–601 (2004).
13. C. Von Sonntag, G. Mark, A. Tauber, and H.-P. Schuchmann, OH radical formation and dosimetry in the sonolysis of aqueous solutions, *Adv. Sonochem.*, No. 5, 109–145 (1999).
14. I. Akhatov, U. Parlitz, and W. Lauterborn, Pattern formation in acoustic cavitation, *J. Acoust. Soc. Am.*, **96**, No. 6, 362–363 (1994).
15. J. B. Keller and M. Miksis, Bubble oscillations of large amplitude, *J. Acoust. Soc. Am.*, **68**, No 2, 628–633 (1980).
16. Z. Dingand and S. M. Gracewski, Response of constrained and unconstrained bubbles polithotripter shock wave pulses, *J. Acoust. Soc. Am.*, **96**, No. 6, 363–364 (1994).
17. W. Lauterborn and U. Parlitz, Methods of chaos physics and their applications to acoustics, *J. Acoust. Soc. Am.*, **84**, No 6, 197–199 (1988).
18. U. Parlitz, V. Englisch, C. Schesczyk, and W. Lauterborn, Bifurcation structure of bubble oscillators, *J. Acoust. Soc. Am.*, **88**, No 2, 1061–1077 (1990).
19. M. A. Diaz de la Rosa, *High-Frequency Ultrasound Drug Delivery and Cavitation: Master Thesis*, Brigham Young University (2007).
20. J. B. Keller and M. Miksis, Bubble oscillations of large amplitude, *J. Acoust. Soc. Am.*, **68**, No. 2, 628–633 (1980).
21. U. Parlitz, Robust method for experimental bifurcation analysis, *Int. J. Bifurcation Chaos*, **12**, No. 8, 1909–1913 (2002).
22. A. A. Koulesoff and V. V. Nelayev, New approach for the response surface methodology, *Proc. SPIE*, **4348**, 435–439 (2001).